Comparative Medicine
Copyright 2015
by the American Association for Laboratory Animal Science

Vol 65, No 5
October 2015
Pages 409–415

Original Research

Evaluation of Nonalcoholic Fatty Liver Disease in C57BL/6J Mice by Using MRI and Histopathologic Analyses

Jae-Eun Ryu,[1] Woori Jo,[1] Hyun-Ji Choi,[1] Sungwoong Jang,[1] Hyo-Ju Lee, [1] Dong-Cheul Woo,[1] Jeong Kon Kim,[3] Kyung Won Kim,[3] Eun Sil Yu,[2] and Woo-Chan Son[1,2,*]

Nonalcoholic fatty liver disease (NAFLD) can lead to cirrhosis, hepatocellular carcinoma, and ultimately death. Magnetic resonance techniques are accurate, noninvasive methods for evaluating hepatic steatosis but, in animals, have not been fully validated against histologic findings. We sought to validate the MRI fat-signal fraction (MRI–FSF) used for diagnosing NAFLD in human nonclinical trials by comparing MRI data with histopathologic findings in C57BL/6J mice (*n* = 24) fed normal chow (controls) or a methionine- and choline-deficient (MCD) diet to induce NAFLD. Axial T2-weighted fast spin-echo images were used to examine the entire liver. For histopathologic analyses, liver slides were evaluated for hepatic steatosis according to the NAFLD activity score. Pearson correlation coefficient and receiver operating characteristics analyses were performed. According to the fat-fraction signal, the mean percentage of liver fat in mice with induced NAFLD was 57%, which correlated with the histologically determined steatosis grade. The proton-density fat fraction effectively distinguished severe from mild hepatic steatosis, with an AUC of 0.92. Evaluation accuracy decreased when lobular inflammation and hepatocellular ballooning were considered. This study showed strong concurrence between MRI–FSF and histopathologic steatosis in a murine model of NAFLD. MRI–FSF had moderate sensitivity and specificity in this context. These results confirm that the MRI is a useful biomarker of hepatic steatosis in NAFLD in murine model.

Abbreviations: FSF, fat-signal fraction; MCD, methionine-and choline-deficient diet; NAFLD, nonalcoholic fatty liver disease.

Nonalcoholic fatty liver disease (NAFLD) is recognized as a clinical state that can develop to end-stage liver disease.[1] This disease eventually can lead to cirrhosis and hepatocellular carcinoma, which in its advanced stage is associated with increased risk of death.[3] The prevalence of NAFLD has increased with the increased adoption of a sedentary lifestyle and changes in dietary habits.[20,29,31,32] Therefore, accurate diagnosis of NAFLD is an important issue. Until recently, liver biopsies were the 'gold standard' for the diagnosis and grading of NAFLD.[5] However, liver biopsy is an invasive method that is inappropriate for screening or frequent monitoring in humans.[9] Likewise, although histopathologic analysis of the liver is the accepted standard for NAFLD grading in animal models, this method is unsuitable for longitudinal studies.[12,24] Many studies have focused on developing accurate, noninvasive tools for the diagnosis of NAFLD.

MRI techniques to noninvasively quantify hepatic steatosis and to analyze other important features of NAFLD in humans have been developed and sufficiently validated through many clinical studies.[4,22,30] However, MRI has not been widely used in preclinical animal studies, mainly because it has not been fully validated against a histopathologic reference.[30] To incorporate MRI in longitudinal animal studies as a means to monitor the degree of hepatic steatosis, the accuracy of MRI techniques to diagnose and grade hepatic steatosis must be validated thoroughly.

To this end, we sought to validate the diagnostic performance of an MR technique in a murine NAFLD model by using histopathologic data as reference standard. Specifically, we aim to evaluate the correlation between the fat fraction estimated by using this MR technique and the histologic grade of hepatic steatosis and the diagnostic accuracy of MRI to differentiate severe steatosis from mild to moderate steatosis. Moreover, we aim to identify any potential factors that might influence the MRI-based estimation of hepatic fat.

Materials and Methods

Animals. We used a murine model in which NAFLD is induced through the administration of a methionine- and choline-deficient diet (Dyets, Bethlehem, PA); this model approximates most of the histologic features of NAFLD.[11,13,18] The MCD diet is high in sucrose and fat and low in methionine and choline. Methionine and choline are essential elements for hepatic β-oxidation and VLDL production.[26] The mice that consume this MCD diet develop severe pericentral steatosis and lobular inflammation with mononuclear and polymorphonuclear infiltration. In addition, the MCD diet impairs mitochondrial β-oxidation and cause

Received: 24 Feb 2015. Revision requested: 08 Apr 2015. Accepted: 03 Jun 2015.
[1]Asan Institute for Life Sciences and [2]Department of Pathology, University of Ulsan College of Medicine and [3]Department of Radiology, University of Ulsan College of Medicine, Asan Medical Center, Seoul 138-736, Republic of Korea
**Corresponding author. Email: wcson@amc.seoul.kr*

http://prime-pdf-watermark.prime-prod.pubfactory.com/ | 2024-12-26

Table 1. Body weight, liver weight (relative to body weight), and blood chemistry (mean ± 1 SD) of mice fed the normal or MCD diet for 8 or 12 wk

	Body weight (g)	Relative liver weight (%)	AST	ALT
8 wk				
Normal chow	30.18 ± 1.06	3.93 ± 0.21	36.12 ± 2.26,	21.17 ± 1.8
MCD diet	19.60 ± 0.30[b]	4.83 ± 0.20[a]	638.8 ± 223.7[a]	450.2 ± 134.0[a]
12 wk				
Normal chow	31.57 ± 0.79	3.51 ± 0.21	141.80 ± 19.54	24.52 ± 3.00
MCD diet	15.59 ± 0.36[b]	4.67 ± 0.41[a]	458.3 ± 48.6[a]	236.7 ± 58.5[a]

[a]Value significantly ($P < 0.005$) different from that for the mice fed the normal diet for the same time period.
[b]Value significantly ($P < 0.0001$) different from that for the mice fed the normal diet for the same time period.

high oxidative stress, mitochondrial DNA damage, and apoptotic cell death, which are important factors in the progression from steatosis to nonalcoholic steatohepatitis.[14,17] C57BL/6 mice (age, 7 wk; Orient Bio, Yongin, Korea) were housed at the laboratory animal facility at the Asan Institute for Life Sciences under SPF conditions. The mice were free of viral pathogens (Sendai virus, mouse hepatitis virus, ectromelia virus, lymphocytic choriomeningitis virus), bacterial pathogens (*Mycoplasma pulmonis*, *Clostridium piliforme*, *Bordetella bronchiseptica*, *Salmonella* spp., *Streptococcus pneumoniae*, *Pasteurella pneumotropica*, *Staphylococcus aureus*, *Citrobacter rodentium*), and parasites (*Eimeria* spp., *Syphacia* spp., and ectoparacites). Cages and bedding were sterilized and changed weekly. The room was kept on a 12:12-h light:dark cycle, at 22 ± 2 °C, and a relative humidity of 55% ± 5%. This study was reviewed and approved by the IACUC of the Asan Institute for Life Sciences, Asan Medical Center (IACUC no. 2014-12-058).

C57BL/6 mice were divided into 4 experimental groups (n = 6 per group) and fed as follows: 1) normal chow for 8 wk, 2) MCD diet for 8 wk, 3) normal chow for 12 wk, and 4) MCD diet for 12 wk. The body weight and food intake of each group were recorded weekly. At the end of the experimental period, mice were evaluated by MRI, weighed, and then euthanized by exsanguination under isoflurane anesthesia. Blood was collected from the inferior vena cava, centrifuged at 2091 × g for 10 min at 4 °C, and serum collected. AST and ALT was determined by using a commercial kit (no. 7180, Hitachi, Tokyo, Japan). Livers were removed rapidly, weighed, and fixed in formalin for histologic analyses.

Tissue processing, histologic analysis, and criteria for pathologic assessment. After 48 h of fixation in 10% neutral buffered formalin, a slice of the median lobe of the liver was trimmed, processed, sectioned into slices approximately 3 µm thick, mounted on a glass slide, and stained with hematoxylin and eosin. Liver sections were examined histopathologically for NAFLD-specific lesions, during which they were blindly evaluated for steatosis, ballooning, and inflammation and thus scored for NAFLD activity. Steatosis was graded as: 0, 0% to 5% of the hepatocytes in the section are steatotic; 1, greater than 5% to 33% of hepatocytes are steatotic; 2, greater than 33% to 66%; and 3, greater than 66%. Ballooning was scored as: 0, absent; 1, mild (focal; involving fewer than 3 hepatocytes); 2, moderate (focal and involving 3 or more hepatocytes or multifocal); and 3, severe (multifocal, with more than 2 foci of 3 or more hepatocytes). Inflammation was graded as: 0, absent; 1, minimal (0 or 1 focus per 20× field); 2, mild (2 foci); 3, moderate (3 foci); and 4, severe (4 or more foci per 20× field). We performed 2 statistical analyses of correlation with MRI findings: one that considered only steatosis when evaluated and another analysis was considered steatosis, inflammation and ballooning degeneration.

MRI to estimate the FSF in liver. MRI was performed by using a 9.4-T, 160-mm small-animal imaging system (Agilent, Palo Alto, CA) with a 30-mm 'millipede' volume coil. For MRI, all mice were anesthetized with 1% to 2% isoflurane in air delivered via a nose cone. Respiratory rate, ECG, and rectal temperature were monitored. To evaluate NAFLD, we adopted an MRI method for calculating the fat-signal fraction (FSF) that includes common fat-suppression techniques to suppress the signal from adipose tissue and chemical shift-based techniques that induce phase differences to allow for more robust water–fat separation. We chose MRI because it is the most widely used technique in clinical practice, and a good correlation between the fat fraction estimated by hepatic MRI and the histologic steatosis grade can be achieved.[25] Axial T2-weighted fast spin-echo imaging (also known as rapid acquisition with relaxation enhancement) was used to scan the entire liver. The parameters of the T2-weighted imaging were: relaxation time, 4000 ms; k_0, 4; echo spacing, 12 ms; 32 segments, echo train length, 8; effective echo time, 48 ms; 2 averages; matrix, 256 × 256; field of view, 25 × 30 mm; slice thickness, 0.8 mm; and total scan time, 4 min 24 s. To measure the fat–lipid signal, both the fat–lipid-saturated and -unsaturated images were acquired, and the off-resonance radiofrequency pulse for the fat–lipid-saturated images was set at 1300 to 1400 Hz from the water signal. For image processing, the region of interest was positioned in the right part of medial lobe that relatively close to the stomach, to avoid motion artifact that made by lung. The signal intensity from nonfat-suppressed images was the sum of the water and fat signals, the signal intensity from fat-suppressed images was the water signal, and the difference in signal intensity between nonfat-suppressed and fat-suppressed images was the fat signal. The fat-fraction signal (η) of the region of interest was calculated as:

$$\eta = \frac{S_{NFS} - S_{FS}}{S_{NFS}}$$

where S_{NSF} is the signal from the nonfat-suppressed images and S_{FS} is that from fat-suppressed images.

Statistical analyses. All results are presented as mean ± 1 SD; differences with a P value of 0.05 or less were considered significant. The estimated FSF was compared between the control group and NAFLD group by using Student t test. The correlation between the FSF and histopathologic grade of hepatic steatosis was determined by using the Pearson correlation coefficient (r^2).

http://prime-pdf-watermark.prime-prod.pubfactory.com/ | 2024-12-26

Table 2. Individual NAFLD activity scores

Mouse	No. of weeks on MCD diet	Score			
		Steatosis	Lobular inflammation	Hepatocyte ballooning	Total
1	8	3	1	1	5
2	8	3	2	1	6
3	8	2	1	1	4
4	8	2	1	2	5
5	8	3	2	2	7
6	8	2	2	1	5
7	12	1	2	2	5
8	12	1	2	2	5
9	12	2	2	2	6
10	12	3	2	2	7
11	12	3	2	2	7
12	12	2	2	1	4

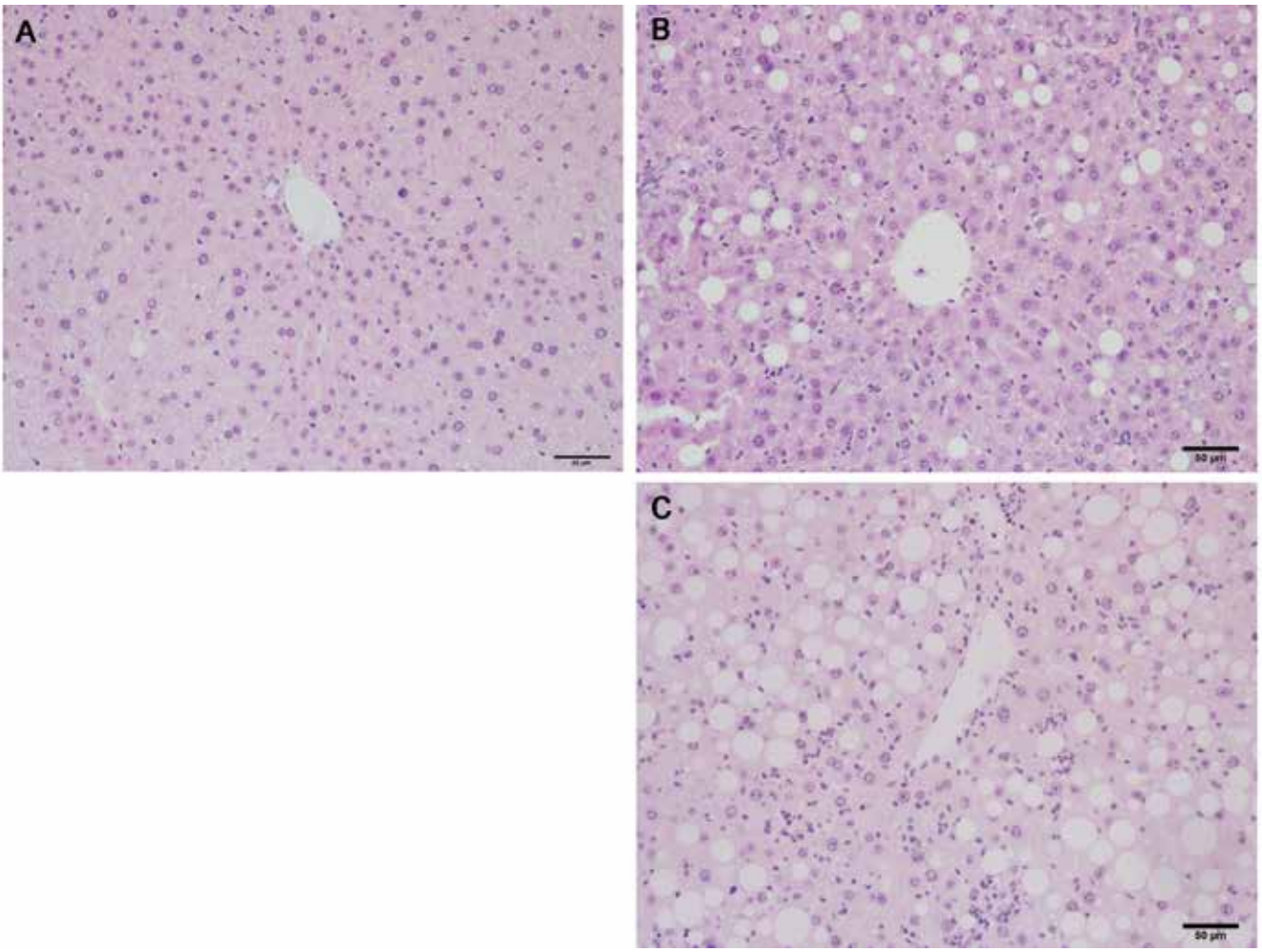

Figure 1. Sections of liver from (A) normal C57BL/6J mice, (B) mice fed an MCD diet for 8 wk, and (C) mice fed an MCD diet for12 wk. Much greater lobular inflammation is present in mice fed MCD for 12 wk (panel C) than for 8 wk (B). Hematoxylin and eosin stain; magnification, 200×.

Receiver operating characteristic (ROC) analysis was used to evaluate the diagnostic performance of MRI–FSF to differentiate severe hepatic steatosis from that mild to moderate in grade. ROC analysis yields a plot of the true-positive rate against the false-positive rate for all possible cut points for a diagnostic test. The area under the ROC curve and 95% confidence interval

http://prime-pdf-watermark.prime-prod.pubfactory.com/ | 2024-12-26

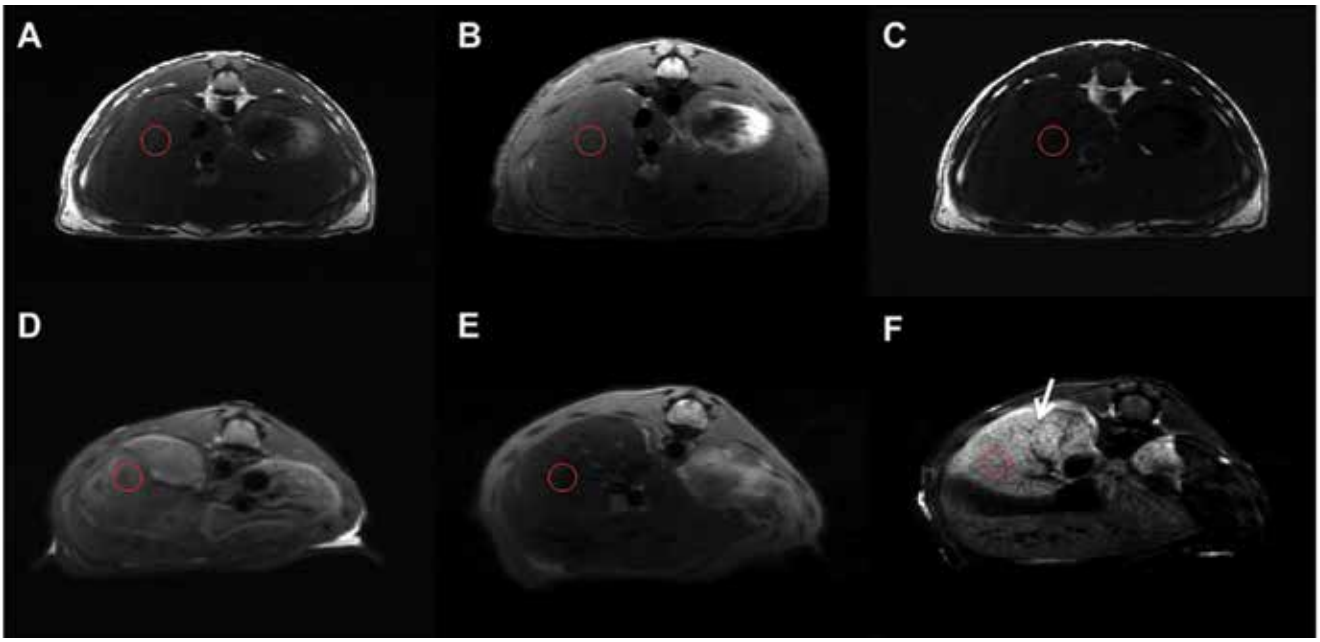

Figure 2. Signal fat-fraction (FSF) obtained using a fat-suppression MRI technique. (A) Images of the liver acquired without fat saturation in normal mice, (B) with fat saturation, (C) MR images acquired as no fat saturation– fat saturation, showingthe fat signal, (D) images of the liver acquired with no fat saturation in mice fed an MCD diet, (E) with fat saturation, (F) MRI fat signals revealed greater fat infiltration in the liver of MCD mice than in that of normal mice (white arrow).

were calculated. The optimal cut-off value of FSF to maximize sensitivity and specificity for differentiating moderate from severe steatosis was determined. For all statistical analyses, Prism 6 (GraphPad Software, La Jolla, CA) was used.

Results

Disease model. The body weight of mice fed an MCD diet was lower ($P < 0.0001$) than that of the normal mice (Table 1). The relative liver weight (%) of mice fed an MCD diet was higher ($P < 0.0001$) than that of mice fed a normal diet (Table 1). Median serum AST and ALT levels (Table 1) of MCD mice were higher ($P < 0.005$) than those of mice fed a normal diet.

Histopathology. The NAFLD activity scores of all mice are presented in Table 2. The livers of MCD mice exhibited more pronounced steatosis, inflammation, and ballooning degeneration of hepatocytes (Figure 1 B and 1 C) than did those of control mice fed a normal diet (Figure 1 A). These histopathologic findings demonstrate that prolonged provision of an MCD diet induced NAFLD in our mice. In terms of hepatic steatosis, 58.3% of the MCD-fed mice had grade 2 lesions, with the remaining 41.3% having grade 3 changes; all normal mice were negative (grade 0) for hepatic steatosis. Lobular inflammation affected the mice with induced NAFLD (grade 1, 25% of the group; grade 2, 75%), but none of the normal mice exhibited any inflammatory foci. Hepatocyte ballooning in NAFLD-induced mice was grade 1 in 41.3% of the mice and grade 2 in 58.3%. Whereas the degree of steatosis did not differ between the mice fed the MCD diet for 8 compared with 12 wk, both inflammation and hepatocyte ballooning were greater in the 12-wk group (Figure 1 B and 1 C, Table 2). We consequently categorized mice according to histologic scores for each feature and then compared these data with the MRI–FSF values.

MRI and the estimated FSF. In all mice, we achieved cross-sectional MRI with high spatial resolution and good image quality. As illustrated in Figure 2, cross-sectional MRI revealed marked lipid infiltration in the livers of NAFLD model mice, whereas little lipid was apparent in the livers of control mice. Subtracting the fat-suppressed images from nonfat-suppressed images (Figure 2) enabled us to evaluate the degree of hepatic steatosis and the distribution of fat infiltration, which is an advantage of MRI over liver biopsy.

The estimated MRI–FSF ranged from 42.5% to 71.5% in NAFLD mice and from 7.7% to 39.3% in normal mice. The mean FSF was higher in NAFLD mice than in control mice: at 8 wk, the FSF of normal liver was 21.74% ± 5.34% but that of NAFLD liver was 64.76% ± 2.69% ($P < 0.005$; Figure 3); this same trend was apparent in the 12-wk groups (control, 25.44% ± 5.81%; NAFLD, 54.18% ± 4.62%; $P < 0.005$, Figure 4).

Correlation of FSF and histologic grade. Pearson correlation (r^2) analysis revealed strong correlation between MRI–FSF and the histopathologic steatosis grade ($r^2 = 0.820$, $P = 0.0053$; Figure 5).

Diagnostic performance of MRI technique. When steatosis was considered, the AUC of the MRI–FSF was 0.92 and the cut-off point measurement was 58.50% (95% confidence interval, 0.7384 to 1.102; $P = 0.0283$, Figure 6) for differentiating moderate from severe steatosis with a sensitivity of 100.0% and a specificity of 80.0%. The cut-off point of the FSF value with the highest specificity (sensitivity; 60%; specificity; 100%) was 67.65%. When lobular inflammation and hepatocellular ballooning were considered in addition to steatosis, the AUC of the MRI–FSF was 0.75 (95% confidence interval, 0.4250 to 1.075; $P = 0.2008$; Figure 7). Under these conditions, the cut-off point was 58.50% to differentiate moderate from severe NAFLD with a sensitivity of 100.0% and a specificity of 66.67%. The cut-off point of the FSF value with the highest sensitivity (sensitivity, 100%; specificity, 66.67%) was the same

http://prime-pdf-watermark.prime-prod.pubfactory.com/ | 2024-12-26

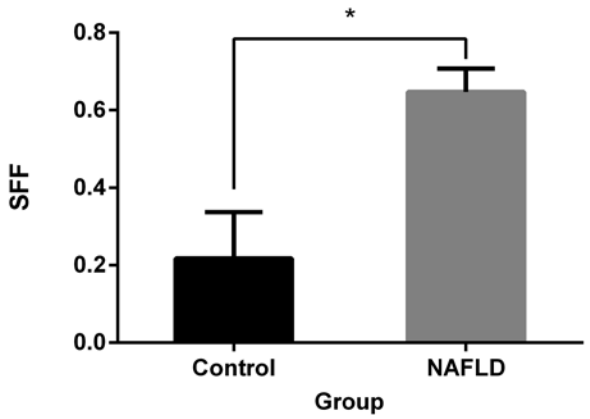

Figure 3. Comparison of normal mice and mice fed an MCD diet for 8 wk. MRI–FSF revealed a greater percentage ($P < 0.0001$) of fat in the livers of MCD mice than in control mice.

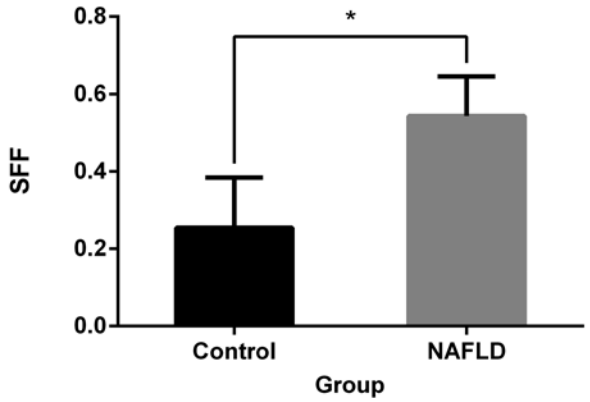

Figure 4. Comparison of normal mice and mice fed an MCD diet for 12 wk. MRI–FSF revealed a greater percentage ($P = 0.0046$) of fat in the livers of MCD mice than in control mice.

as the cut-off point with the highest specificity (sensitivity, 50%; specificity, 83.33%), which was 67.65%.

Discussion

This study demonstrated the value of the MRI–FSF index in the diagnosis of NAFLD in murine models by using histopathologic analysis as a reference standard.

The MRI–FSF revealed large differences in lipid content (percentage) in the liver of control mice and those with NAFLD, suggesting that MRI–FSF provides good diagnostic accuracy for quantifying steatosis. However, MRI–FSF measured a maximum fat content of 39.3% in the livers of normal mice, whereas these mice exhibited a lipid content of only 5% in the histopathologic analysis. This erroneous estimate of hepatic fat content was produced by using fat-suppression MRI techniques. Incomplete fat saturation and inadvertent water suppression are potential risk factors (disadvantages) of using fat-suppression MRI techniques.[25] We observed a close correlation between the MRI–FSF and the grade of steatosis as determined by histopathologic results ($r = 0.820$, $P = 0.0053$). The MRI–FSF generally increased with a higher histologically determined steatosis grade. This result suggests that several potential factors (lobular inflammation, hepatocellular ballooning, and nonalcoholic steatohepatitis) did not greatly affect the correlation between MRI–FSF and the histologic steatosis grade in the current study.

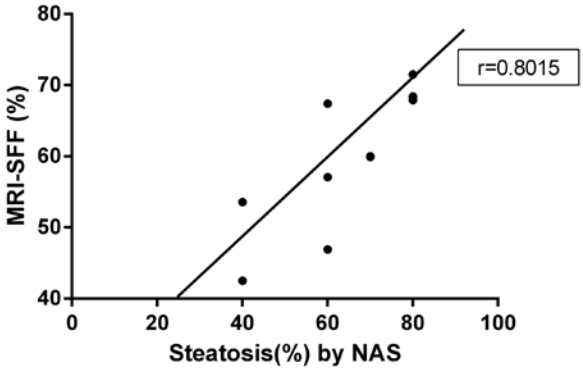

Figure 5. In liver with induced NAFLD, MRI–FSF measurements of hepatic fat content (%) and histologic measurements of steatosis (%) are highly correlated ($P = 0.0053$).

The MR–FSF differentiated severe steatosis from mild or moderate steatosis in our murine model, with 100.0% sensitivity and 80.0% specificity. However, when lobular inflammation and hepatocellular ballooning were included with steatosis, the AUC decreased. This decreased sensitivity and specificity indicated that MRI techniques based only on fat content had a limited ability to evaluate NAFLD. It is important to note that MRI shows the proportion of protons that are in a lipid environment compared with an aqueous environment,[25] whereas pathologic analyses measure the number of hepatocytes that show lipid vacuolation or inflammatory and degenerative changes. NAFLD should be differentiated from steatosis, with or without hepatitis. Although the quantity of lipid in the liver is an important feature, the degree of inflammation is integral to the diagnosis of NAFLD as well.[1] Therefore MRI that is based on solely on calculating of the quantity of hepatic lipid is problematic when establishing an accurate diagnosis of NAFLD, and additional markers or MR techniques are required to evaluate nonlipid factors, such as fibrosis or inflammation in nonalcoholic steatohepatitis.[6,27]

Several recent studies have demonstrated the value of MRI, particularly its noninvasiveness, for diagnosing various diseases, assessing the efficacy or toxicity of a drug, and tracing tumor progression in animal models.[2,8,28,33] For example, iron oxide-enhanced MRI has been used to evaluate the phagocytic activity in atherosclerotic plaques in mice treated with irbesartan, an antagonist of the angiotensin II receptor that may decrease atherosclerotic lesion formation.[28] Another study evaluated the ability of MR techniques to identify subtle metabolic disorders induced by antipsychotic drugs in C57BL6 mice.[2] Other MR techniques need to be validated for proving their value in other medical applications.

Prior studies evaluated the correlation between histologic results and MRI–MR spectroscopy data in a rodent NAFLD model.[7,15,19,21,34] According to one report,[34] in vivo proton MR spectroscopy enabled the noninvasive assessment of hepatic lipid levels and, as a result of its high spectral resolution, yielded information regarding fat composition. Another study[21] found that the preenhancement fat-fraction ratio on T2-weighted images was a useful measurement for estimating the progression of liver fat deposition and fibrosis in nonalcoholic steatohepatitis and

http://prime-pdf-watermark.prime-prod.pubfactory.com/ | 2024-12-26

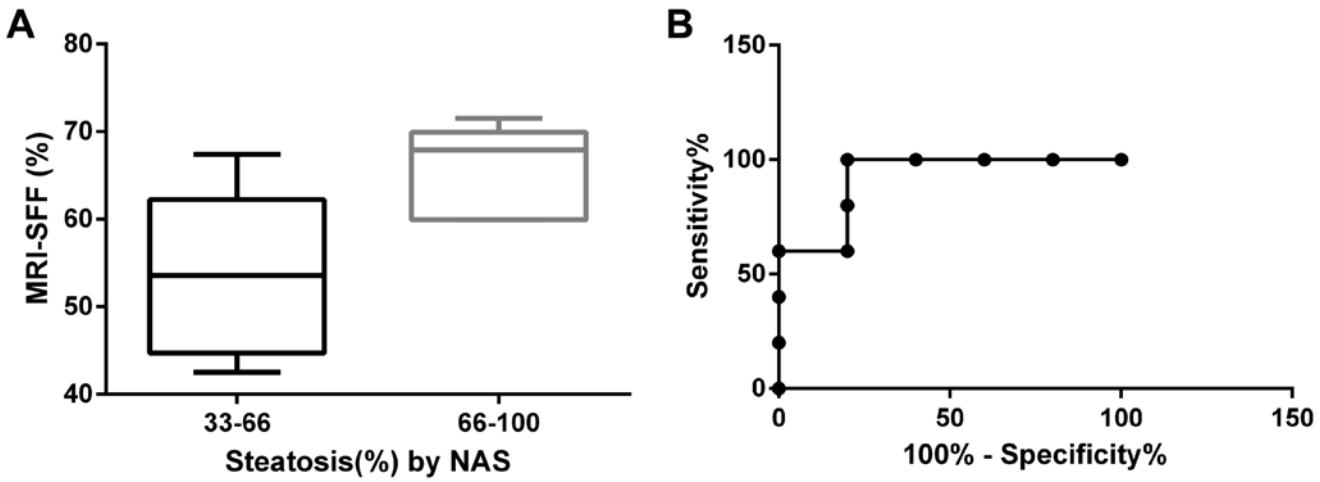

Figure 6. Receiver operating characteristic analysis of MRI–FSF and the histologically determined grade of steatosis for mice with induced NAFLD. MRI–FSF can distinguish between histologic degrees of steatosis: moderate (33% to 66%) and severe (66% to 100%) hepatic steatosis. (B) Receiver operating characteristic curve of MRI–FSF for steatosis.

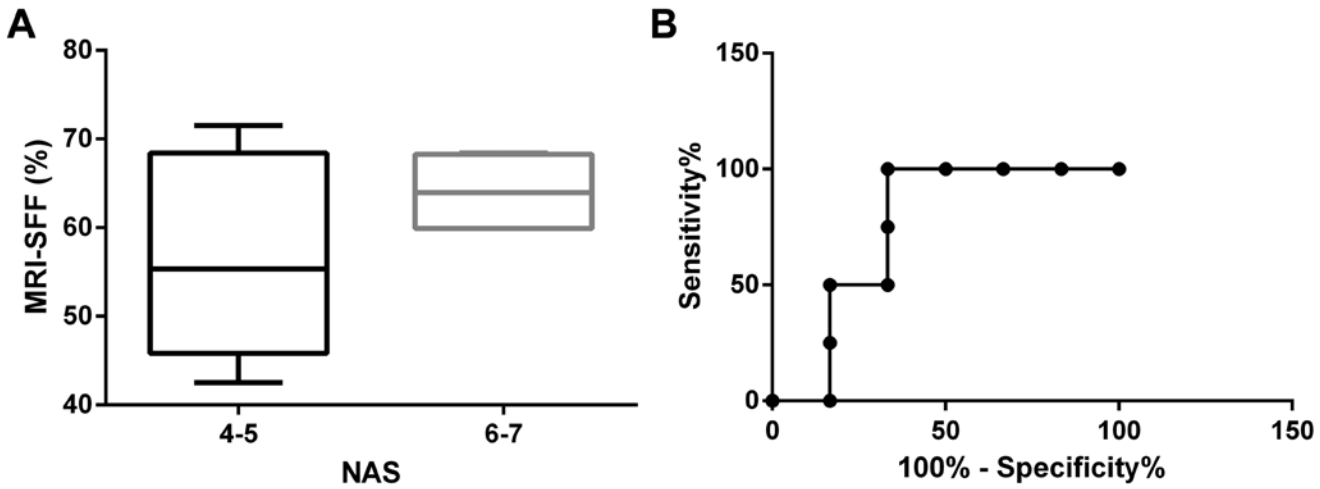

Figure 7. Receiver operating characteristic analysis of MRI–FSF for histologically determined NAS grades for mice with NAFLD. (A) MRI–FSF discriminates between moderate (score; 4 to 5) and severe (score; 6 to 7) NAS grade. (B) The receiver operating characteristic curve for NAS grade showed a lower sensitivity and specificity than that for steatosis.

identified a relationship between the histologic grade and the fat-fraction ratio obtained by MRI. Other colleagues[19] reported that hepatic fat content as determined by proton MR spectroscopy was highly correlated with histologic determinations of steatosis in a rat MCD model and that MR spectroscopy accurately distinguished between degrees of clinical steatosis. In addition, several human studies have evaluated the correlation between histologic findings and MRI.[10,16,23] The identification of markers that can be used in clinical trials is a very important issue for the development of new therapeutics; thus our current study provides a useful reference. Our findings are in agreement with those of previous studies, and our current study is the first to demonstrate that the evaluation accuracy of MRI–FSF decreased when estimating the correlation between all three NAFLD activity scores.

One limitation of our study is that MCD diets induce malnutrition and subsequent weight loss in mice,[14] whereas most humans with nonalcoholic steatohepatitis are obese and insulin-resistant. Therefore this represents an important difference between the mouse MCD model and human nonalcoholic steatohepatitis. Another limitation is that the grade of steatosis was higher than expected. That is, none of our MCD-fed mice exhibited minimal steatosis (5% to 20%). Given that feeding durations of 1, 2, 3, and 5 wk have been recommended previously,[19] the 8- and 12-wk durations we used may have been too long.

In conclusion, this study demonstrated concurrence between MRI–FSF and histopathologic steatosis in a murine model of NAFLD. MRI–FSF provided an accurate estimation of the presence of hepatic steatosis and was diagnostically valuable for distinguishing between mild and severe forms of hepatic steatosis in a murine model. MRI–FSF showed moderate sensitivity and specificity. These results would confirm that MRI is a useful diagnostic marker of hepatic steatosis during NAFLD in a murine model.

http://prime-pdf-watermark.prime-prod.pubfactory.com/ | 2024-12-26

Acknowledgments

This research was supported by grant no. HI14C1090 from the Korea Health Technology R&D Project through the Korea Health Industry Development Institute (KHIDI), funded by the Ministry of Health and Welfare, Republic of Korea. In addition, this study was supported by grants (nos. HI06C0868 and HI10C2014) from the Korean Health Technology Research and Development Project, Ministry of Health and Welfare, Republic of Korea.

References

1. **Angulo P.** 2002. Nonalcoholic fatty liver disease. N Engl J Med **346:**1221–1231.
2. **Auger F, Duriez P, Martin-Nizard F, Durieux N, Bordet R, Petrault O.** 2014. Long-term risperidone treatment induces visceral adiposity associated with hepatic steatosis in mice: a magnetic resonance approach. Schizophr Res Treatment **2014:** 1–11.
3. **Bjornsson E, Angulo P.** 2007. Nonalcoholic fatty liver disease. Scand J Gastroenterol **42:**1023–1030.
4. **Bohte AE, van Werven JR, Bipat S, Stoker J.** 2010. The diagnostic accuracy of US, CT, MRI, and ^{1}H-MRS for the evaluation of hepatic steatosis compared with liver biopsy: a meta-analysis. Eur Radiol **21:**87–97.
5. **Bravo AA, Sheth SG, Chopra S.** 2001. Liver biopsy. N Engl J Med **344:**495–500.
6. **Chen J, Talwalkar JA, Yin M, Glaser KJ, Sanderson SO, Ehman RL.** 2011. Early detection of nonalcoholic steatohepatitis in patients with nonalcoholic fatty liver disease by using MR elastography. Radiology **259:**749–756.
7. **Corbin IR, Furth EE, Pickup S, Siegelman ES, Delikatny EJ.** 2009. In vivo assessment of hepatic triglycerides in murine nonalcoholic fatty liver disease using magnetic resonance spectroscopy. Biochim Biophys Acta **1791:**757–763.
8. **Fan X, Mustafi D, Markiewicz E, Zamora M, Vosicky J, Leinroth A, Mueller J, Macleod K, Conzen SD, Karczmar GS.** 2014. Mammary cancer initiation and progression studied with magnetic resonance imaging. Breast Cancer Res **16:**495.
9. **Gaidos JK, Hillner BE, Sanyal AJ.** 2008. A decision-analysis study of the value of a liver biopsy in nonalcoholic steatohepatitis. Liver Int **28:**650–658.
10. **Idilman IS, Aniktar H, Idilman R, Kabacam G, Savas B, Elhan A, Celik A, Bahar K, Karcaaltincaba M.** 2013. Hepatic steatosis: quantification by proton-density fat fraction with MR imaging versus liver biopsy. Radiology **267:**767–775.
11. **Itagaki H, Shimizu K, Morikawa S, Ogawa K, Ezaki T.** 2013. Morphological and functional characterization of non-alcoholic fatty liver disease induced by a methionine–choline-deficient diet in C57BL/6 mice. Int J Clin Exp Pathol **6:**2683–2696.
12. **Kn BP, Gopalan V, Lee SS, Velan SS.** 2014. Quantification of abdominal fat depots in rats and mice during obesity and weight-loss interventions. PLoS One **9:**e108979.
13. **Koteish A, Diehl AM.** 2001. Animal models of steatosis. Semin Liver Dis **21:**89–104.
14. **Lee HS, Son WC, Ryu JE, Koo BA, Kim YS.** 2014. Standardized *Salvia miltiorrhiza* extract suppresses hepatic stellate cell activation and attenuates steatohepatitis induced by a methionine–choline-deficient diet in mice. Molecules **19:**8189–8211.
15. **Levene AP, Kudo H, Armstrong MJ, Thursz MR, Gedroyc WM, Anstee QM, Goldin RD.** 2012. Quantifying hepatic steatosis—more than meets the eye. Histopathology **60:**971–981.
16. **Ligabue G, Besutti G, Scaglioni R, Stentarelli C, Guaraldi G.** 2013. MR quantitative biomarkers of non-alcoholic fatty liver disease: technical evolutions and future trends. Quant Imaging Med Surg **3:**192–195.
17. **Liu Y, Song H, Wang L, Xu H, Shu X, Zhang L, Li Y, Li D, Ji G.** 2014. Hepatoprotective and antioxidant activities of extracts from *Salvia–Nelumbinis naturalis* against nonalcoholic steatohepatitis induced by methionine- and choline-deficient diet in mice. J Transl Med **12:**315.
18. **London RM, George J.** 2007. Pathogenesis of NASH: animal models. Clin Liver Dis **11:**55–74 [viii.].
19. **Marsman HA, van Werven JR, Nederveen AJ, Ten Kate FJ, Heger M, Stoker J, van Gulik TM.** 2010. Noninvasive quantification of hepatic steatosis in rats using 3.0-T ^{1}H-magnetic resonance spectroscopy. J Magn Reson Imaging **32:**148–154.
20. **Matteoni CA, Younossi ZM, Gramlich T, Boparai N, Liu YC, McCullough AJ.** 1999. Nonalcoholic fatty liver disease: a spectrum of clinical and pathological severity. Gastroenterology **116:**1413–1419.
21. **Okada M, Katsube T, Kumano S, Kagawa Y, Araki T, Tsuda N, Okuaki T, Imaoka I, Tanigawa N, Ishii K, Murakami T.** 2011. Unenhanced fat fraction ratios obtained by MR and enhanced T2* values with liver-specific MR contrast agents for diagnosis of nonalcoholic steatohepatitis in rats. Acta Radiol **52:**658–664.
22. **Pais R, Pascale A, Fedchuck L, Charlotte F, Poynard T, Ratziu V.** 2011. Progression from isolated steatosis to steatohepatitis and fibrosis in nonalcoholic fatty liver disease. Clin Res Hepatol Gastroenterol **35:**23–28.
23. **Permutt Z, Le TA, Peterson MR, Seki E, Brenner DA, Sirlin C, Loomba R.** 2012. Correlation between liver histology and novel magnetic resonance imaging in adult patients with nonalcoholic fatty liver disease—MRI accurately quantifies hepatic steatosis in NAFLD. Aliment Pharmacol Ther **36:**22–29.
24. **Polyzos SA, Mantzoros CS.** 2014. Necessity for timely noninvasive diagnosis of nonalcoholic fatty liver disease. Metabolism **63:**161–167.
25. **Reeder SB, Cruite I, Hamilton G, Sirlin CB.** 2011. Quantitative assessment of liver fat with magnetic resonance imaging and spectroscopy. J Magn Reson Imaging **34:**729–749.
26. **Rinella ME, Elias MS, Smolak RR, Fu T, Borensztajn J, Green RM.** 2008. Mechanisms of hepatic steatosis in mice fed a lipogenic methionine choline-deficient diet. J Lipid Res **49:**1068–1076.
27. **Salameh N, Larrat B, Abarca-Quinones J, Pallu S, Dorvillius M, Leclercq I, Fink M, Sinkus R, Van Beers BE.** 2009. Early detection of steatohepatitis in fatty rat liver by using MR elastography. Radiology **253:**90–97.
28. **Sigovan M, Kaye E, Lancelot E, Corot C, Provost N, Majd Z, Breisse M, Canet-Soulas E.** 2012. Antiinflammatory drug evaluation in ApoE$^{-/-}$ mice by ultrasmall superparamagnetic iron oxide-enhanced magnetic resonance imaging. Invest Radiol **47:**546–552.
29. **Sugino H, Kumagai N, Watanabe S, Toda K, Takeuchi O, Tsunematsu S, Morinaga S, Tsuchimoto K.** 2008. Polaprezinc attenuates liver fibrosis in a mouse model of nonalcoholic steatohepatitis. J Gastroenterol Hepatol **23:**1909–1916.
30. **Tang A, Tan J, Sun M, Hamilton G, Bydder M, Wolfson T, Gamst AC, Middleton M, Brunt EM, Loomba R, Lavine JE, Schwimmer JB, Sirlin CB.** 2013. Nonalcoholic fatty liver disease: MR imaging of liver proton density fat fraction to assess hepatic steatosis. Radiology **267:**422–431.
31. **Teli MR, James OF, Burt AD, Bennett MK, Day CP.** 1995. The natural history of nonalcoholic fatty liver: a follow-up study. Hepatology **22:**1714–1719.
32. **Vizzutti F, Provenzano A, Galastri S, Milani S, Delogu W, Novo E, Caligiuri A, Zamara E, Arena U, Laffi G, Parola M, Pinzani M, Marra F.** 2009. Curcumin limits the fibrogenic evolution of experimental steatohepatitis. Lab Invest **90:**104–115.
33. **Wada T, Miyashita Y, Sasaki M, Aruga Y, Nakamura Y, Ishii Y, Sasahara M, Kanasaki K, Kitada M, Koya D, Shimano H, Tsuneki H, Sasaoka T.** 2013. Eplerenone ameliorates the phenotypes of metabolic syndrome with NASH in liver-specific SREBP1c Tg mice fed high-fat and high-fructose diet. Am J Physiol Endocrinol Metab **305:**E1415–E1425.
34. **Ye Q, Danzer CF, Fuchs A, Wolfrum C, Rudin M.** 2012. Hepatic lipid composition differs between ob/ob and ob/+ control mice as determined by using in vivo localized proton magnetic resonance spectroscopy. MAGMA **25:**381–389.

http://prime-pdf-watermark.prime-prod.pubfactory.com/ | 2024-12-26